Iraqi Geological Journal

Journal homepage: https://www.igj-iraq.org

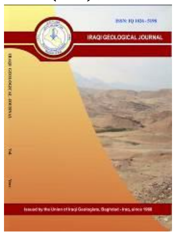

Jeed Formation (Upper Maastrichtian–Lower Danian) Western Iraq: A New Siliceous-Phosphatic Lithostratigraphic Unit

Ibrahim Q. Mohammed[1] **and Anwar K. Mousa**[2]

1 Al Salam University College, Baghdad, Iraq
2 Department of geology, College of science, University of Baghdad, Baghdad, Iraq
* **Correspondence**: anwar.mousa@sc.uobaghdad.edu.iq

Received:
23 March 2026
Accepted:
16 July 2026
Published:
31 August 2026

Abstract

The Jeed Formation (Upper Maastrichtian to Lower Danian) in the Western Desert of Iraq is a new proposed mixed lithostratigraphic succession containing various rock types, including phosphatic, siliceous, calcareous, siliciclastic, and other mineralogical contents (carbonate flouraptite, quartz, calcite, dolomite, opal-CT, smectite, palygorskite, sepiolite, kaolinite, and locally zeolite). The current study presents a review compliant with ICS standards and a revised lithostratigraphic framework for the Jeed Formation, based on a synthesis of historical usage, stratigraphic evolution, and previous miscorrelations, along with contributions from new data from integrated lithological, mineralogical, and microfacies datasets. The formation has been formally redefined and recognized as the correct stratigraphic unit, thus replacing the earlier misapplied Upper Campanian-Lower Maastrichtian Digma Formation in Western Iraq. The Jeed Formation consists of two members: the Upper Maastrichtian Safra Member and the Lower Danian Trafawi Member, each subdivided into two beds: lower and upper. The upper Maastrichtian member shares the same depositional phase as the lower Danian member, with a symmetrical lithological architecture and comparable depositional basins, indicating a series of identical lithofacies controlled by regional and continental factors rather than local ones. The Cretaceous-Paleogene (K/Pg) transition is marked by a geologically significant unconformity that extends across the entire region and serves as a marker for the Safra /Trafawi member boundary. Regional correlation between the Muwaqqar Chalk Marl Formation of Jordan, the Jalamid Formation of northern Saudi Arabia, and the Dakhla Formation of Egypt highlights the role of the Jeed Formation within a continuous Maastrichtian–Danian phosphogenic belt along the southern margin of the Tethys Ocean.

Keywords: Jeed Formation; Western Desert; Wadi Trafawi; Lower Danian; Rutbah

1. Introduction

The Western Desert of Iraq hosts an important lithologically similar Maastrichtian-Lower Danian mixed marine succession comprising phosphatic, siliceous, siliciclastic, and carbonate deposits. It records the continuation of phosphate-rich greenhouse conditions from the Late Cretaceous into the Paleogene along the southern Tethyan margin. Although regionally significant, the lithostratigraphy of this succession has been complicated by conflicting correlations with the Tayarat and Digma formations. Early research, such as Van Bellen et al., 1959; Al-Naqib, 1967; Buday & Hak, 1980, linked the phosphorite layer to the Upper Campanian-Maastrichtian Tayarat Formation, placing it within a shallow-marine Upper Cretaceous Rutbah Basin (Fig. 1). A significant shift occurred when Buday & Hak, 1980, proposed linking the continental–marine transition siliciclastic–dolomitic succession north and west of the Ga'ara Depression with the deep-marine Upper Campanian-Lower Maastrichtian fine-grained limestone and marly limestone with glauconite and phosphate Digma Formation in the Anah Graben. This connection relates continental deposits and tidal shallow-marine mixed siliciclastic-carbonate facies to deep-marine marl–limestone deposits of varying ages. Fossil assemblages, depositional environments, and tectonic contexts have contributed to long-standing stratigraphic discrepancies. In 1984, Jassim and colleagues introduced the Jeed Formation to represent the distinct Maastrichtian phosphatic deposits in Wadi Jeed and nearby areas. However, later stratigraphic studies such as Jassim and Buday in Jassim & Goff, 2006; Sissakian & Mohammed, 2007; Al-Bassam, 2017; Sissikian & Fouad, 2016, without justification for the low of the international stratigraphic law and rock unit classification, dismissed the Jeed Formation, as well as the Safra Unit. Digma Formation was documented only in the Anah-1 borehole (Van Bellen et al., 1959; Mohammed, 1993 in Mohammed et al. (2022). It is known to represent an Upper Campanian–Lower Maastrichtian deep-marine *Globotruncana aegyptica* Zone succession (Al-Mutwaily, 1992), with no lithological or biostratigraphic equivalence to units of the Western Desert (Mohammed, 1993 in Mousa et al. (2021). It is essential to note that the previously recognized Safra unit was Late Maastrichtian and was subsequently replaced by the Digma Formation, which is Late Campanian to Early Maastrichtian. Extensive field observations (1982–2023), petrographic, and microfacies investigations (more than a thousand thin sections and 200 samples for clay stratigraphy), reported by Mohammed (1993) in Mohammed et al. (2022) conclusively demonstrate that the Western Desert phosphatic succession is not Digma Formation but a regionally mappable Upper Maastrichtian-Lower Danian inner to upper ramp marine system (Figs. 1–6). It comprises two genetically linked members: Upper Maastrichtian Safra Member, Lower Danian Trafawi Member, separated by a hiatus of variable duration across the K/Pg transition within the exposed successions and boreholes (Mohammed et al., 2022) (Fig. 4). These findings justify reinstating the Jeed Formation in accordance with International Commission on Stratigraphy(ICS) guidelines and provide a more precise framework for its lithostratigraphic definition and paleoenvironmental interpretation.This study aims to formally re-establish the Jeed Formation as the accurate lithostratigraphic unit for the Upper Maastrichtian-Lower Danian phosphatic, siliceous, siliciclastic, and carbonate mixed succession in the Western Desert of Iraq, following the standards and nomenclatural principles of the International Commission on Stratigraphy (ICS). As well as to develop a consistent depositional paleoenvironmental model for the Jeed paleoenvironmental model for the Jeed Formation establish strong regional correlations with coeval units in Jordan, Saudi Arabia, and Egypt. model for the Jeed Formation

2. Materials and Methods

The current study presents a review compliant with ICS standards combines field observations (1982–2023), lithological documentation, microfacies analysis, and clay mineralogical data (more than a thousand thin sections and 200 samples for clay stratigraphy) petrographic to clarify the internal subdivision of the succession into the Safra and Trafawi members, define its stratigraphic boundaries, and distinguish it from the deep-marine Upper Campanian–Lower Maastrichtian Digma Formation (Figs. 3 and 4).

The biostratigraphic scheme used in this study is based on the lowest occurrence (LO) and highest occurrence (HO) of bioevents in planktic foraminifera, using the charts of Wade et al. 2011. The sequence stratigraphy used in this study follows the concepts and terminology of Catuneanu (2017), with an emphasis on sequence boundaries (SB) and systems tracts. Moreover, the regional sequence stratigraphy chart of the Arabian Plate by Sharland et al. (2001) is used. The classification of lithofacies and microfacies is based on grain composition, texture, and structure are classified using different schemes (Dunham, 1962; and Embry and Klovan, 1971).

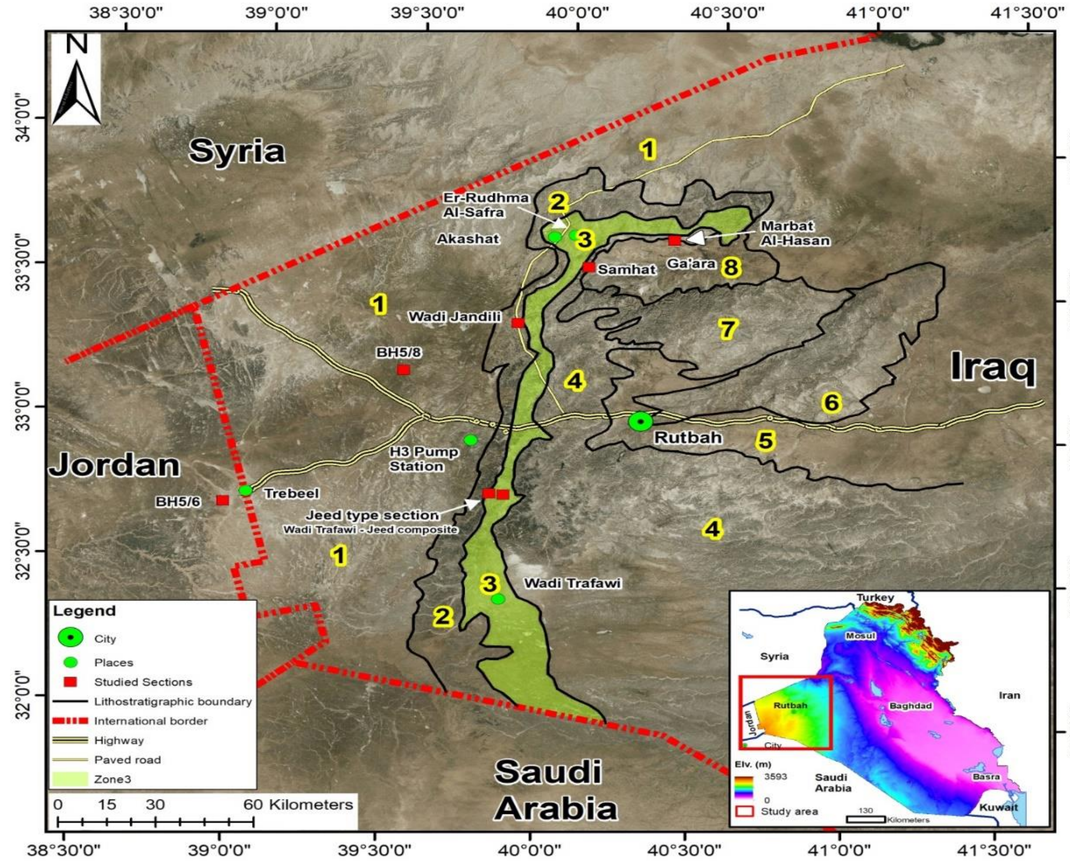

Fig.1. Landsat image showing the locations of the analyzed sections and a simplified distribution of several rock units in the Western Desert of Iraq. 1 = Eocene Ratgha Formation; 2 = Upper Danian-Thanetian Akashat Formation; 3 = Maastrichtian-Lower Danian Jeed Formation; 4 = Upper Campanian-Maastrichtian Tayarat Formation; 5 = Cenomanian strata; 6 = Jurassic strata; 7 = Triassic strata; 8 = Permian strata. The inset location map shows a digital elevation model and the position of the Western Desert of Iraq (Modified after Mohammed et al., 2022)

Age/Stage	Van Bellen et al. (1959)	Buday and Hak (1980)	Jassim et al. (1984)	Al-Bassam et al. (1990)	Mohammed (1993)	This study
Selandian	Umm Er Radhuma /Semhat Fm. (Phosphatic facies)	Umm Er Radhuma Fm.	Akashat Fm.	Akashat Fm.: Hirri Mb.	Akashat Fm.: Upper	Akashat Fm.: Hirri Mb.
Danian				Akashat Fm.: Trafawi Mb.	Akashat Fm.: Lower	Jeed Fm.: Trafawi Mb.
Maastrichtian	Tayarat Limestone	Tayarat: Upper / Lower	Jeed/Tayarat	Jeed / Tayarat - Hartha: Safra Mb.; Na'ajha / Marbat Mbs.	Jeed/Tayarat	Jeed Fm.: Safra Mb.; Tayarat Fm.
Campanian		Digma Fm.	Hartha; Samhat Fm.	Jeed / Tayarat - Hartha: Na'ajha / Marbat Mbs.	Jeed/Tayarat	Tayarat Fm.
Santonian						
Coniacian						
Turonian		Ms'ad Fm.	Ms'ad - Rutbah Fms.	Ms'ad - Rutbah Fms.	Ms'ad Fm.	
Cenomanian	Ms'ad Fm.; Rutbah Sandstone	Rutbah Sandstone	Ms'ad - Rutbah Fms.	Ms'ad - Rutbah Fms.	Rutbah Sandstone	Ms'ad - Rutbah Fms.

Fig. 2. Existing lithostratigraphic classification and our revised proposal for the Upper Cretaceous sequence in the Western West-Rutbah region

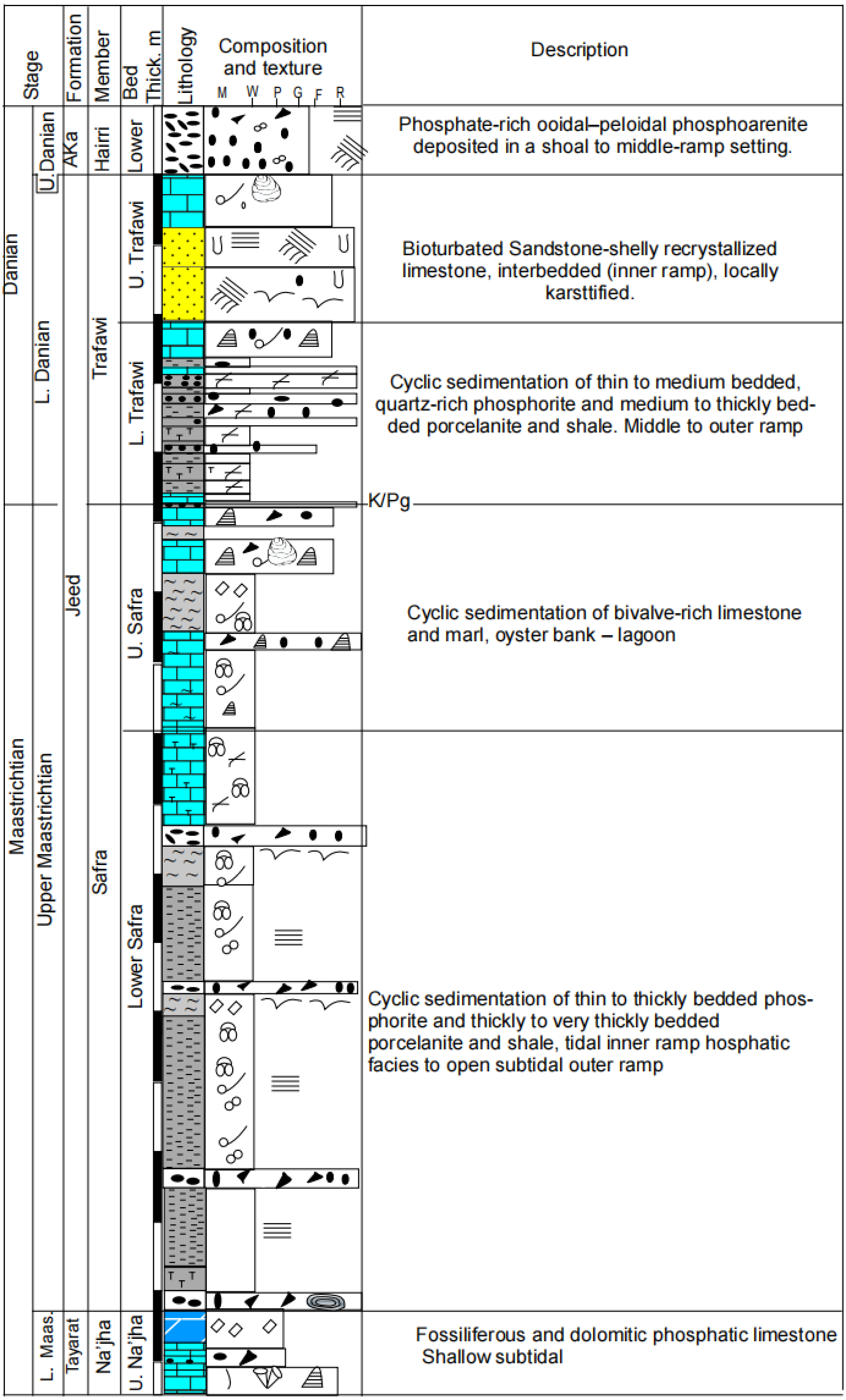

Fig. 3. Lithostratigraphic, texture composition, and detailed description of the Jeed Formation in the studied section

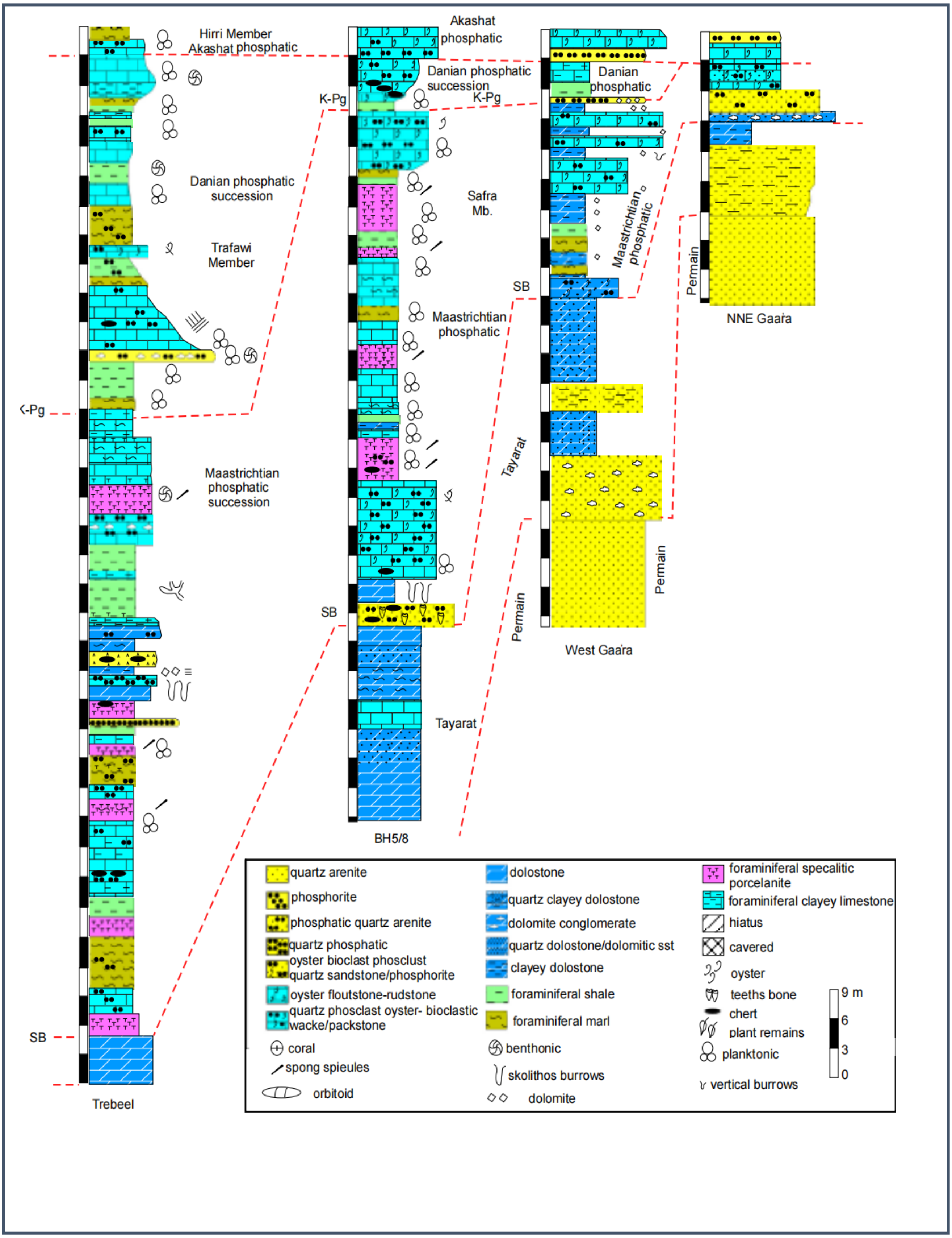

Fig.4. Stratigraphic correlation of the examined successions, illustrating the distribution of lithofacies

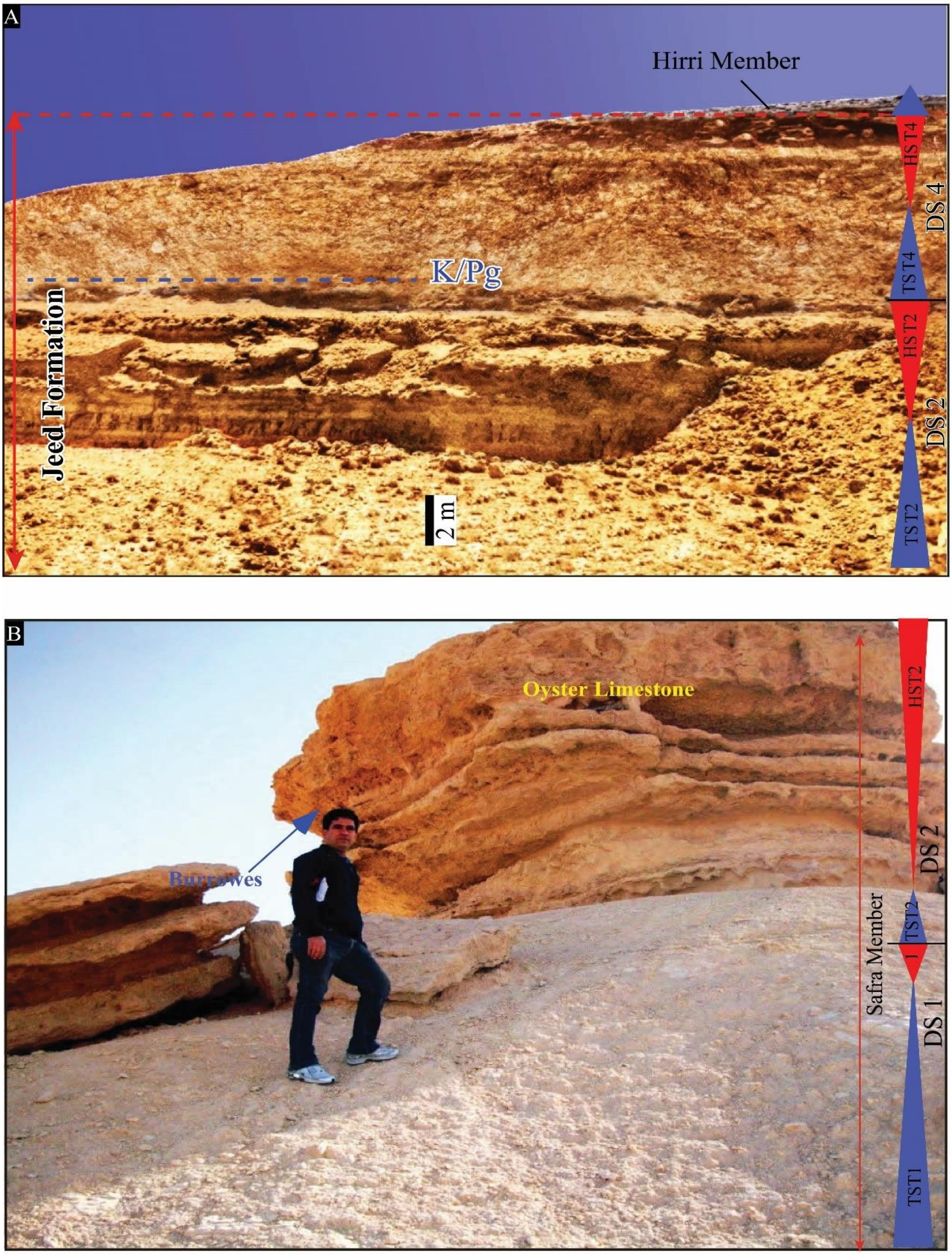

Fig. 5. A) Displays a field photo of the Upper Maastrichtian Safra (TST2 and HST2) and Danian Trafawi (TST4/HST4) members of the Jeed Formation, pointing out the location of the K/Pg unconformity at the Wadi Trafawi section. B) Field photo showing the lower shale-marl layers (TST1), followed by burrowed dolomitic marl (HST1), phosphatic marl (TST2), and oyster-rich limestone (HST2) of the Safra Member at Er-Rudhma Al-Safra Hill (Mohammed et al., 2022).

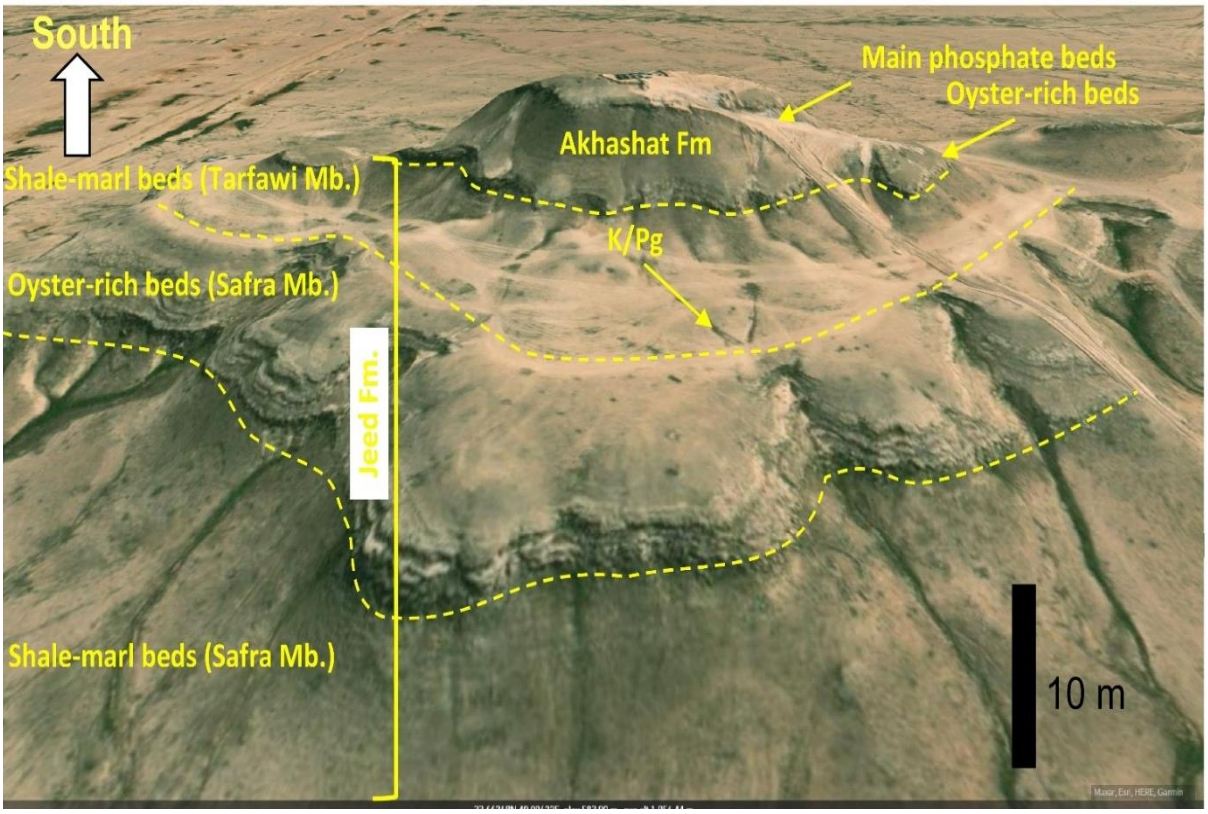

Fig.6. Oblique satellite imagery from Google Maps depicting the lithofacies of the Safra Member (Up per Maastrichtian) and the Lower Danian Trefawi Member (Jeed Formation), beside the phosphoriteri ch Upper Danian Hiri Member (Akashat Formation) lithofacies. The section's height is around 40 m

3. Results

3.1. Formal Lithostratigraphic Definition

3.1.1. Type and reference sections

The Upper Maastrichtian–Lower Danian Jeed Formation is prominently exposed in Wadi Jeed in the Western Desert. Its composite stratotype, defined from Wadi Jeed and Wadi Trafawi, includes the complete Safra–Trafawi succession and the K/Pg boundary. The formation has a wide distribution in the western part of Iraq within Marbat – Trabeel Basin, like Tel Al-Safra, Marbat El-Hosan, Wadi Samhat, Wadi Jandili, and boreholes BH5/6 and BH5/8 (Fig. 7) . The type section of the Jeed Formation is located at the confluence of Wadi Jeed and Wadi Trafawi, which provides the most complete and representative exposure of the succession. The locality lies about 60 km southwest of Rutbah City, 20 km south of the H3 pumping station, and approximately 130 km south of the Akashat Mine (32°24′06.54″N, 39°51′12.08″E) (Fig. 1). The succession exposed in Wadi Jeed (32°34′06.56″N, 39°50′53.51″E) is included to complete the stratigraphic record (Fig. 1). Supplementary reference sections, particularly for the lower part of the succession, are well exposed near the type section in the Bshira Mine area, located ~40 km south of H3 and ~85 km southwest of Rutbah City. Other reference sections include Er-Rudhma Al-Safra (40°02′08″N, 33°40′35″E), which lies east of the Akashat Phosphate Mine, and Wadi Jandili (39°51′12″N, 33°21′51″E). These sections primarily document the Safra Member and are crucial for recording its lateral variability and facies evolution. For the Trafawi Member, Wadi Trafawi (32°24′06″N, 39°51′12″E) is the best type area because it exhibits the full stratigraphic succession.

3.1.2. Lithology, boundaries, and thickness

The Jeed formation begins with a basal layer of phosphorite, phosphatic sandstone, and conglomerate, followed by spiculitic porcellanite, chert, carbonaceous shale, smectite-rich marl and shale, foraminiferal to marly limestone, dolomite, dolomitic sandstone, and oyster-rich limestone. Its lower boundary is an unconformity on the Tayarat with the underlying Tayarat Formation (Lower Maastrichtian). At the same time, the upper boundary is also an unconformity with the overlying Akashat Formation (Upper Danian–Thanetian), locally marked by karst Features. The Jeed Formation consists of two members: the Safra Member (Upper Maastrichtian) and the Trafawi Member (Lower Danian). Thickness in the type area is 48.85 and the formation showing high lateral variations in thickness ranges from approximately 9.75 in the northeast Ga'ara Depression to 87 near the Trabeel area and 107 m along the western flank of Rutbah High.

Measured type of the Jeed Formation, showing the composite succession in Wadi Jeed and Wadi Trafawi, located approximately 60 km southwest of Rutbah City and 20 km south of H3 Pumping Station. Coordinates: (32°24′06.54″N, 39°51′12.08″E)

- Akashat Formation, Hirri Member: ovoidal phosphorie, …………. +2.00

Sequence boundary

- Jeed Formation, Trafawi Member, Upper Trafawi bed :

42. limestone, thick-bedded, light gray with reddish soil, bivalve – bearing, highly recrystallized, and locally karstified ………………………… +1.65

41. Sandstone, yellowish gray, thick-bedded, laminated with low-angle cross bedding, rounded, coarse-grained, well-sorted, *Scolithos* burrows …… 2.90

40. Sandstone, gray, thick-bedded, laminated to cross-laminated, moderate bioturbation, *Thalassinoides*-dominated, rounded, coarse sand, moderate sorting, phosphatic with sparry–calcite cement …………………… 1.00

39. Sandstone, gray, thick-bedded, complete bioturbation, *Thalassinoides* burrows, coarse sand, rounded, medium sorting. ………………… 1.40

38. Limestone, gray to yellowish brown, thick-bedded, bivalve shell fragments, highly recrystallized, with chert lenses. Floatstone texture…….. 1.50

37. Sandstone, yellowish brown, laminated, small cross-laminated, rounded, medium sand, moderate bioturbation to coarse sand, well sorted. 0.20

36. Shale, calcerous, greenish to dark gray, laminated, sharp contact with the sandstone above …………… 0.60

35. Phosphorite, dark gray, hybrid arenite (phosphatic bone m coprolite, peloids, quartz, iron pisods, clay, and foraminifera) ……………… 0.15

Jeed Formation, Trafawi Member, Lower Treafawi bed

34. Porcellanite, dark gray, massive, sharp boundaries, upper surface highly bioturbated and filled with phosphatic grains. Wackestone texture 0.25

33. Phosphorite, dark gray, thin layer, bone, coprolite, intraclasts, quartz, bivalve fragments, and foraminifera, hybrid arenite, poorly sorted 0.05

32. Porcellanite, dark gray, phosphatic, clayey, and wackestone texture 0.15

31. Phosphorite, dark gray, hybrid arenite ……………………………… 0.15

30. shale, black, calcerous and phosphatic, fissile, fibrous calcite…..0.60

29. Sandstone, gray, fine sand, subrounded, poor-sorting, iron-pisoids – bearing…………………0.10

28. Porcellanite, dark gray, clayey-phosphatic- chertitified and small light color geodes, carbonaceous, gradational with underlying phosphate. 0.95
27. Phosphorite, gray, mixed with porcellanite, fibrous calcite crystals 0.07
26. Shale, green to dark gray, sandy at the upper part, laminated, fibrous calcite crystals with a waxy appearance …………………………… 0.90
25. Porcellanite, gray, clayey, phosphatic, quartz, *Thalassinoides* burrows back-filling by quartz sand………………………………………………0.70
24. Shale, green to gray, fissile………………………………………………0.15
23. Porcellanite, dark-gray, clayey…………………………………………0.27
22. hybrid porcellanite-clay – phosphate-quartz at the erosional surface of the K/Pg boundary; the porcellanite is white and light, burrows filled by quartz and phosphate. 0.12
21. Phosphorite; quartz-sand – rich, subrounded, poor-sorting, coarse sand, Thalaassinoides back-filling, rests directly on the irregular surface……………………………………………… …………… 0.05-0.30

Erosional surface and Major sequence boundary K/Pg

- Jeed Formation, Safra Member, Upper Safra Member:

20. Limestone, creamy, hard, oyster-pelecypod, gastropods, shells, fragments, phosphate bone coprite intraclasts bioturbation burros infilling by quartz and phosphate sand, floatstone texture………………………1.00
19. Marl, yellowish brown to gray, laminated, massive, ornamented by Thalassinoides burrows at the top……..0.70
18. Limestone, yellowish gray, thick bedded, locally cross-bedded, large fossil fragments rich (oyster, pelecypod, gastropod, algae, phosphatic bone), highly recrystallized, calcirudite, angular to subangular, poorly sorted, floatstone to rudstone texture……………………..1.30
17. Marl, light gray with yellowish brown irregular structure may be weathering, massive, occasionally laminated, the upper 20-30 cm with Thalassinoides burrows filled by phosphatic and shell fragments display firmground surface ………………..2.10
16. Limestone, yellowish light gray, large fossil fragments -rich, bivalve, gastropod articulated and disarticulated, detrital older bioclasts (Tayarat Formation), coral, algae, rudist, Loftusia claystone lenses ……………………………………….0.90
15. Marl, yellowish, laminated, hard, with iron-bedded, topped by *Thalassinoides* burrows, erosional surface …………….0.75
14. Limestone, dark gray, massive, cacirudite, sunagular to angular, poorly sorted, silicified, oyster, pelecypod, gastropod, sharp teeth and bone, fragmented, articulated and disarticulated, finning upward from rudstone to floatstone, irregular lower surface and upper surface horizontal and smooth with marl bolls 5 cm diameter and white color…0.50
13. Marl, same above marl, with 5% fossils, erosional upper surface, grains filled *Thalassinoides* burrows …..0.50
12. Limestone, same above, silica Geodes …………0.55
11. Marl, same above………………………………………0.30

- Jeed Formation, Safra Member, Lower Safra bed:

10. Limestone interbedded with porcelanite displays three cycles

The limestone is light gray, thickly bedded, fine-grained, chaky mudstone, marly. The Porcellanite, light gray to white, thick-bedded, massive, light-weight, slightly phosphatic …………90

9. Phosphorite brown to light gray, medium bedded, massive, hybrid arenite to rudite, phosphatic bone, coprolite, lithoslats, bivalve shell fragments, subangular to subrounded, poorly sorted, rudstone phosphorite interbedded with floatstone – packstone phosphatic limestone ……………… 1.2

8. Marl, light brown, massive, laminated, phosphate and bioclasts back-filled *Thalassionides* burrows ……………1.50

7. Shale, yellowish brown to green, fissile, calcerous, occasionally marly. 4.0

6. Phosphorite, gray, medium bedded, bone and coprolite, shell fragments, rudite, subangular to sunrounded …………………………0.90

5. Shale, yellowish brown to green, changes to marl upward ……..7.0

4. Phosphorite, gray, bone coprolite rudite, poorly sorted ………………0.75

3. Shale, yellowish brown to green, fissile ………………3.0

2. Porcellanite, white to light gray, massive, hard, lightweight, locally silicified, clayey and calcerous……1.5

1. Phosphorite, gray, massive, hybrid arenite to rudite, phosphatic bone and coprolite, and bivalve shell fragments and quartz sand in sparry calcite ….0.5

- Tayarat Formation, Na'aja Member:

- Dolomitic limestone, topped by an erosional surface and major sequence boundary ………1.5
- Phosphatic Limestone …………………………0.5
-Limestone………………………………………… 2.0

3.1.3. internal subdivision

The formation is subdivided into the Safra Member and the Trafawi Member, each member subdivided into two beds: lower and upper**.** The Safra Member represents the upper Maastrichtian part of the Jeed Formation, as defined by high-resolution stratigraphic measurements (Fig. 3), extending into the Lower and Upper Safra Beds. The Lower Safra Bed begins with basal phosphorite, phosphatic sandstone, or hybrid arenite containing phophosclasts, calc-bioclasts, and siliciclasts, which overlie the Lower Maastrichtian section of the Tayarat Formation across an erosional contact. Above this lag, the succession includes well-sorted granular phosphorites, spiculitic porcellanite, foraminiferal limestone, and carbonaceous shale in the Trabiel. In contrast, the outcrop sections around the northern and western edges of the Ga'ara Depression and west and southwest of Rutbah City consist of dolomitic ochre shales along the outcrops and carbonaceous calcitic shale to marl in subsurface sections, marly dolomite, and dolomitic marl, interbedded with meter-thick beds of phosphorite or hybrid arenite. The Upper Safra Bed, represented by oyster limestone, is locally bony coprolitic–bearing, interbedded with dolomitic marl and marly dolomite, indicating a gradual shallowing toward inner-ramp environments. Microfacies observations in the lower bed reveal outer-ramp, low-energy environments with abundant planktonic foraminifera and sponge spicules at the base, transitioning upward into the upper bed microfacies, where the mid-ramp phosphatic wackestone and inner-ramp bioclastic and dolomitic deposits predominate. The clay mineral assemblages are mainly composed of smectite and opal-CT in the outer-ramp facies and become gradually enriched in palygorskite and dolomite higher up, implying a shift from a humid–warm to a more semi-arid climate. The Safra Member primarily corresponds to DS1 and DS2 in the sequence-stratigraphic framework and encompasses the Upper Maastrichtian maximum flooding surface and the Lower Danian flooding surface, as well as DS3 and DS4 (F.3) (Mohammed et al., 2022).

The Trafawi Member forms the lower Danian part of the Jeed Formation. It sharply overlies the K/Pg boundary. The Lower Trafawi Bed is marked by a phosphatic firmground with an associated lag of pebbles, phosphatic intraclasts, and bioturbation structures rich in *Thalassinoides* burrows, overlain by porcellanite and green shale in the outcrops and black shale in the boreholes. The succession of the lower bed consists of 5 to 6 depositional cycles of phosphorite-porcellanite – shale cycle. The Upper Trafawi Bed culminating in highly bioturbated sandstone and highly recrystallized, karstic limestone. The lower part of Trafawi indicates a renewed transgression after the end-Cretaceous extinction, followed by gradual shoaling into mid- and inner-ramp facies. Mineralogically, Trafawi shows higher amounts of smectite, opal-CT, quartz, and calcite, suggesting humid climatic conditions. The Trafawi Member corresponds to DS4 in the sequence-stratigraphic scheme and is truncated at the top by the Lower Danian-Upper Danian unconformity (SB5), which marks the upper boundary of the Jeed Formation (Mohammed et al., 2022). In the subsurface study (BH 5/6, an example), the Paleocene succession is inferred to have a conformable K/Pg contact, based on the absence of sedimentological breaks or erosional surfaces and a continuous biostratigraphic record; however, no boundary is observed. Further work is required on the K/Pg boundary in the surface section.

3.2. Biostratigraphy

Three foraminiferal biozones were recorded in the studied Late Maastrichtian succession, and four foraminiferal Paleocene biozones were recognized as follows:

3.2.1. Pseudoguembelina hariaensis Partial Range Zone (CF3).

Definition: The interval from the first Occurrence (FO) of *Pseudoguembelina hariaensis* Nederbragt to the Last Occurrence (LO) of *Gansserina gansseri* Bolli.

Age: Middle Late Maastrichtian, spanning approximately 66.83 Ma to 65.45 Ma.

Assemblages: Includes the index taxon, along with planktonic species such as *Abathomphalus mayaroensis* Bolli, *Globotruncana aegyptiaca* Nakkady, *Globotruncanita stuarti* de Lapparent, and *Rugoglobigerina rugosa* Plummer. Associated benthic foraminifera include *Anomalinoides pinguis* Jennings, *Bolivina incrassata* Reuss, and *Cibicides* sp.

Correlation: This zone is comparable to the *P. hariaensis* (CF3) Partial Range Zone reported globally in regions like Tunisia, the South Atlantic (DSDP Site 525A) (Li and Keller, 1998 b), and Egypt (Keller, 2004), Western Iraq (Mousa,2020 in Mousa et al., 2021). It is also equivalent to the middle part of the *Abathomphalus mayaroensis* zone in Northeast Iraq (Abdel-Kireem, 1997).

3.2.2. Pseudoguembelina palpebra Partial Range Zone (CF2).

Definition: The interval between the LO of *Gansserina gansseri* Bolli. at the base and the FO of *Plummerita hantkeninoides* Brönnimann at the top.

Age: Late Maastrichtian, spanning approximately 65.45 Ma to 65.30 Ma.

Assemblages: Species are generally similar to the underlying CF3 zone, with the addition of *Globotruncana falsocalcarata* Kerdany & Abdelsalam.

Correlation: This zone is comparable to the *P. palpebra* Brönnimann & Brown Zone in the South Atlantic (DSDP Site 525A) (Li & Keller, 1998a), Tunisia (Li and Keller, 1998 b), in Egypt (Farouk et al., 2020), and Western Iraq (Mousa,2020 in Mousa et al., 2020). It is also equated with the *Abathomphalus mayaroensis* zone, which has been reported from multiple locations, including Spain (Canudo et al., 1991) and Italy (Premoli Silva & Sliter, 1995).

3.2.3. Plummerita hantkeninoides Total Range Zone (CF1).

Definition: Marked by the total range of the nominate taxon and the LO of all tropical species, indicating the mass extinction at the Cretaceous/Paleogene (K/T) boundary.

Age: Latest Maastrichtian, spanning approximately 65.30 Ma to 65.00 Ma.

Assemblages: Characterized by abundant and diversified planktonic foraminifera. Most planktonic species continue from CF2, with the addition of *Globotruncanita conica* White. The assemblage includes the index species, *P. hantkeninoides* Brönnimann, along with *Abathomphalus mayaroensis* and *Pseudoguembelina palpebra*.

Correlation: This zone is comparable to the *P. hantkeninoides* (CF1) Zone documented in Tunisia (Li and Keller, 1998 b) and Egypt (El-Younsy et al., 2017), as well as to the Eastern Tethys (Keller, 2004). It corresponds to the highest part of the *Abathomphalus mayaroensis* zone, as identified in various international studies. The top of this zone aligns with the abrupt disappearance of the Maastrichtian planktonic foraminiferal assemblages.

3.2.4. Guembelitria Cretacea Interval Zone (P0).

Definition: Denotes the Cretaceous/Paleocene boundary, described as the interval between the latest appearance of Maastrichtian foraminifera (top of CF1) and the FO of *Parvularugoglobigerina eugubina* Luterbacher & Premoli Silva

Age: Earliest Paleocene (Danian), spanning approximately 65.00 Ma to 64.97 Ma.

Correlation: This zone is equivalent to the *G. cretacea* zone documented in Tunisia (Li and Keller, 1998b), Egypt (El-Younsy et al., 2017), and Northern Iraq (Sharbazheri, 2007), Western Iraq (Mousa et al., 2021).

3.2.5. Parvularugoglobigerina eugubina Total Range Zone

Definition: Delineated by the total range of the index taxon, *P. eugubina* Luterbacher & Premoli Silva.

Age: Earliest Paleocene (Danian), spanning approximately 64.97 Ma to 64.90 Ma.

Assemblages: Includes the index species, along with *Chiloguembelina midwayensi* Cushman, *Globoconusa daubjergensis* Brönnimann, and *Parasubbotina pseudobulloides* Plummer. Associated benthic foraminifera include *Gavelinella danica* Brotzen.

Correlation: This zone is comparable to the *P. eugubina* Zone in Tunisia (Li and Keller, 1998b), Egypt (El-Younsy et al., 2017), Spain (Smit, 2005), and the Eastern Tethys (Keller, 2004).

3.2.6. Parasubbotina pseudobulloides Interval Subzone (P1a).

Definition: The interval between the LO of *P. eugubina* Luterbacher & Premoli Silva and the FO of *Subbotina triloculinoides* Plummer.

Age: Early Paleocene (Early Danian), spanning approximately 64.90 Ma to 64.50 Ma.

Assemblages: Dominant species include *Chiloguembelina midwayensi* Cushman, *Globoconusa daubjergensis* Brönnimann, and *Woodringina hornerstownensis* Olsson.

Correlation: This subzone is comparable to the lower part of the *Morozovella pseudobulloides* Plummer Zone (Bolli, 1966) and the P1a Subzone reported in Tunisia (Arenillas et al., 2002) and Egypt (Keller, 2004; Abu Shama et al, 2026).

3.2.7. Subbotina triloculinoides Interval Subzone (P1b).

Definition: The interval between the FO of *Subbotina triloculinoides* Plummer and the FO of *Globanomalina compressa* Plummer and/or *Praemurica inconstans* Subbotina.

Age: Early Paleocene (Early Danian), spanning approximately 64.50 Ma to 63.00 Ma.

Assemblages: Characterized by the appearance of *Subbotina triloculinoides* Plummer, along with *Chiloguembelina midwayensi* Cushman and *Globoconusa daubjergensis* Brönnimann. *Eoglobigerina simplicissma* Blow is absent.

Correlation: This subzone is comparable to the upper part of the *Morozovella pseudobulloides* zone (Bolli, 1966)

Additional Paleocene Subzone.

Globanomalina compressa / *Praemurica inconstans* - *Praemurica uncinata* Interval Subzone (P1c)

Definition: The interval between the FO of *Globanomalina compressa* Plummer and/or *Praemurica inconstans* Subbotina and the FO of *Praemurica uncinata* Bolli at the top.

Age: Early Paleocene (Early Danian).

Correlation: This subzone is comparable to the *Morozovella trinidadensis* Bolli Zone (Bolli, 1966) and the P1c Subzone of the standard scheme.

3.3. Microfacies and Facies Architecture

Six lithofacies, including phosphorite, hybrid arenite, sandstone, porcelanite (including chert), and shale-to-marl limestone, are part of fifteen microfacies (Mohammed et al., 2022) identified within the Jeed Formation. These microfacies are grouped into three significant facies associations representing outer-, mid-, and inner-ramp settings. The outer ramp association features carbonaceous shale and marl with planktonic foraminifera (Fig. 7A), spiculitic porcellanite containing abundant silica from sponge spicules (Fig. 7B), and dolomitic laminated marl/shale (Fig. 7C). The mid ramp includes phosphatic wackestone, carbonate breccia, and conglomerate (Fig. 7D), ooidal and peloidal phosphorite(Fig. 7E and 7F), foraminiferal wackestone, and bioturbated quartz arenite. These facies reflect higher-energy, storm-influenced environments characterized by repeated reworking and the concentration of phosphatic and siliciclastic grains. The inner ramp comprises oyster floatstone–rudstone (Fig. 7I), bone–coprolite phosphorite (Fig. 7G), dolomitic mudstone, quartz arenite, quartz – bone phosphorite (Fig. 7H), and firmground-associated levels (Fig. 7E), indicating conditions ranging from very shallow marine to intermittently emergent. Collectively, these microfacies demonstrate a fully developed distally steepened ramp profile and allow detailed reconstruction of lateral facies changes across the Western Desert (More detailed descriptions of all sedimentary facies and microfacies of the Jeed Formation succession can be found in (Mohammed et al., 2022).

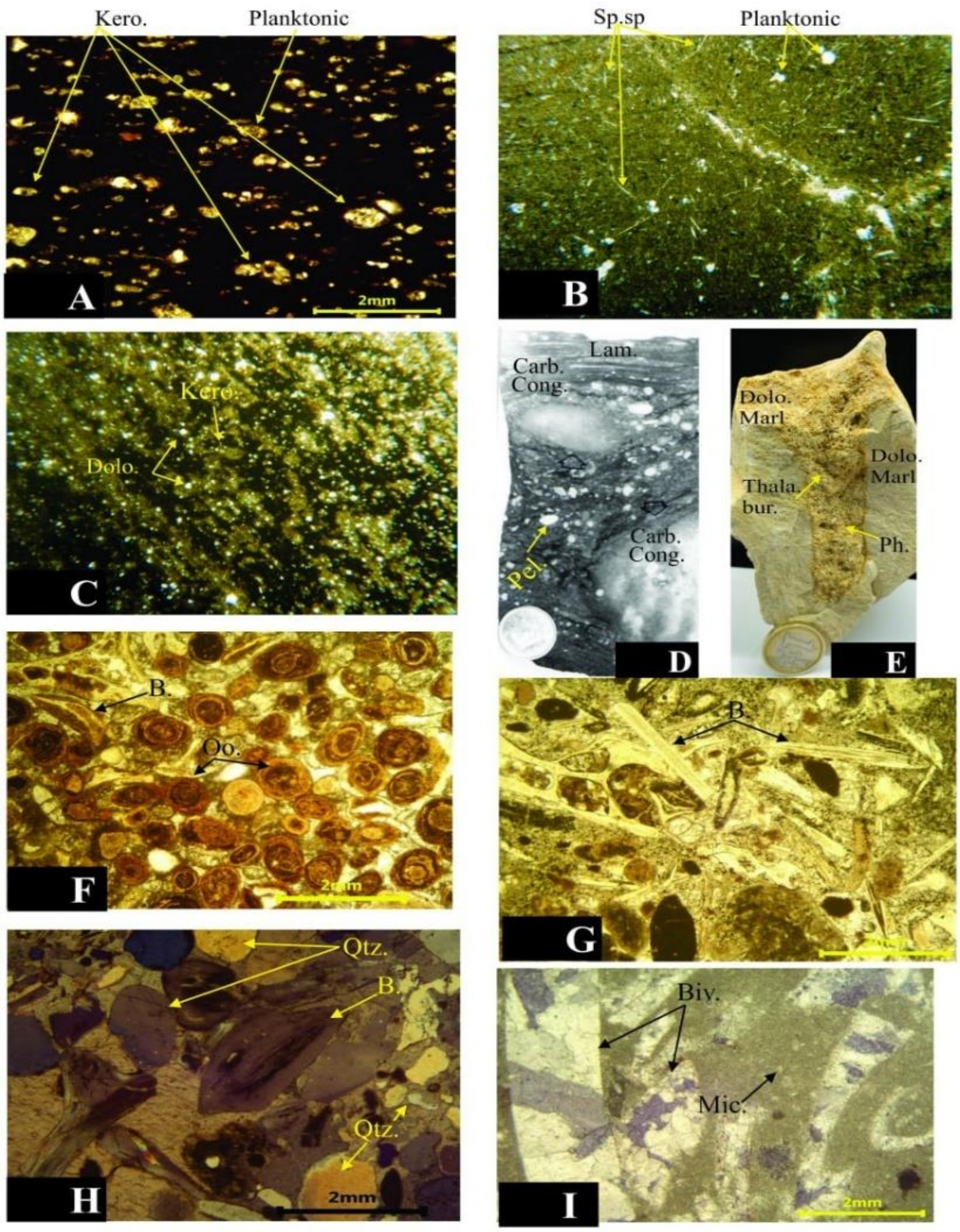

Fig.7. Photomicrographs of the main litho-microfacies of the Jeed Formation under transmitted light, showing sedimentary textures. A) Carbonaceous shale is rich in planktic foraminifera, has a wackestone texture, and is embedded in a carbonaceous, muddy matrix. B) Opal-CT porcellanite with planktic and sponge spicules – rich microcrystalline muddy matrix. C) Dolomitic, laminated marl/shale. D) Phosphatic and foraminiferal-rich- rich fine-grained limestone with carbonate gravel debris, exhibiting finning upward to laminated fine-grained limestone. E) Dolomitic marl with hybrid arenite (phosclasts, bioclasts, quartz sand) filling *Thalassinoides* Burrows. F) Ooidal phosphorite with grain-support, packstone to grainstone texture with some bone fragments. G) Bone coprolite phosphorite with packstone to rudstone texture. H) Hybrid arenite including bone fragments, quartz sand, and sparite cement matrix within a floatstone to rudstone texture. I) Bivalve–rich limestone, micritic matrix filling the pores between the skeletal accumulations, within a floatstone to rudstone matrix. Kero= carbonaceous material ; Plank.F=planktic foraminifera ; Sp.sp=sponge spicules; Dol=dolomite ; Carb.cong=Carbonate conglomerate ; Pel= phosphatic peloids ; Dol.marl = dolomitic marl ; ph = phosphate – rich hybrid arenite ; Th.burr= *Thalassinoides* burrows; Oo=phosphatic ooides ; B=bone fragmentes ; Cop=coprolite ; Qtz=quartz sand ; Biv=bivalve skeletons ; Mic=micrite .

3.4. Clay Minerals Identification

The Maastrichtian–Lower Danian successions (Jeed Formation) of the Marbat-Trabeel Basin exhibit a unique mineralogy, including carbonate flourapatite, quartz, calcite, dolomite, opal-CT, smectite, palygorskite, sepiolite, kaolinite, and, locally, zeolite. The clay mineral assemblage indicates fluctuations in depositional conditions, paleoclimate, and relative sea-level change within a distally steepened marine ramp system. High-resolution X-ray diffraction (XRD) examinations across the basin reveal that smectite and palygorskite are the most common clay minerals (Fig. 8). Kaolinite, sepiolite, illite, and chlorite are present only in small amounts. Smectite is the most common clay mineral in the successions we examined, particularly in fine-grained outer-ramp lithofacies, including black shale, marl, lime mudstone, and porcellanite. The clay fraction comprises 61-100 wt% of it, and the smectite–rich illite–smectite mixed layers (R0 I/S) are the most common type. The smectite has low to moderate crystallinity and broad, asymmetric XRD reflections (Fig. 8), suggesting that it is derived primarily from detrital sources, consistent with previous SEM and TEM investigations (Mohammed et al., 2022). These traits indicate a land-source area that was chemically weathered in a warm, subhumid climate with little topographic relief (Chamley, 1989). The material was then transported over long distances in suspension and deposited in distant marine settings (Mohammed, 1993; Mohammed et al., 2022). From a clay-stratigraphic perspective, smectite is most common in transgressive systems tracts (TSTs) and maximum flooding surfaces (MFSs). This distribution indicates that there was sufficient accommodation space and calm conditions for sediment to settle, resulting in lower hydrodynamic energy and a finer-grained sediment supply as sea level rose. As a result, intervals rich in smectite are good signs of transgressive phases and wetter paleoclimatic conditions. Palygorskite, on the other hand, is more likely to form in shallow-marine inner-ramp facies and regressive highstand systems tracts (HSTs), where it can make up 90–100% of the clay percentage in some places. The stratigraphic rise of palygorskite is linked to elevated Mg and Si in pore fluids, strong dolomitization, and conditions that promote evaporation, all of which are common in shallow, confined marine environments that formed as sea level fell (Chamley, 1989). Kaolinite is present along the proximal inner ramp, and illite is present only in minor to negligible quantities. It is viewed as a detrital constituent, originating from weathered continental sediments or the reworking of earlier siliciclastic formations found in adjacent uplifted source regions. The vertical alternation between smectite-dominated and palygorskite-dominated clay assemblages establishes a resilient clay stratigraphic framework that documents cyclic transgressive–regressive processes, paleoclimatic fluctuations, and basin development during the Maastrichtian–Early Danian period.

In contrast, the clay mineral assemblage of the Digma Formation is dominated by illite and illite–smectite mixed-layer minerals (R0 ordering) (Mohammed, 1993; Mohammed et al., 2022). This assemblage closely resembles that of the lower parts of the Tayarat and Shiranish formations, which are of similar age. Nevertheless, the clay minerals of the Jeed, Akashat, and Ratgha Formations differed in their paleoclimate and sedimentation conditions. The illite–smectite (R0) and palygorskite association indicates a shallow-marine environment with warm conditions and alkaline, magnesium-rich seawater, likely in confined or marginal-marine settings. On the other hand, the R0–illite assemblage points to a mixture of an arid climate at the source, low Mg availability, and a deep-marine depositional environment (Mohammed, 1993; Mohammed et al., 2022).

Accordingly, the marked difference in clay mineral assemblages provides a robust mineralogical criterion for distinguishing the Digma Formation from the Jeed Formation, supporting their separation as stratigraphically and paleoenvironmentally distinct units.

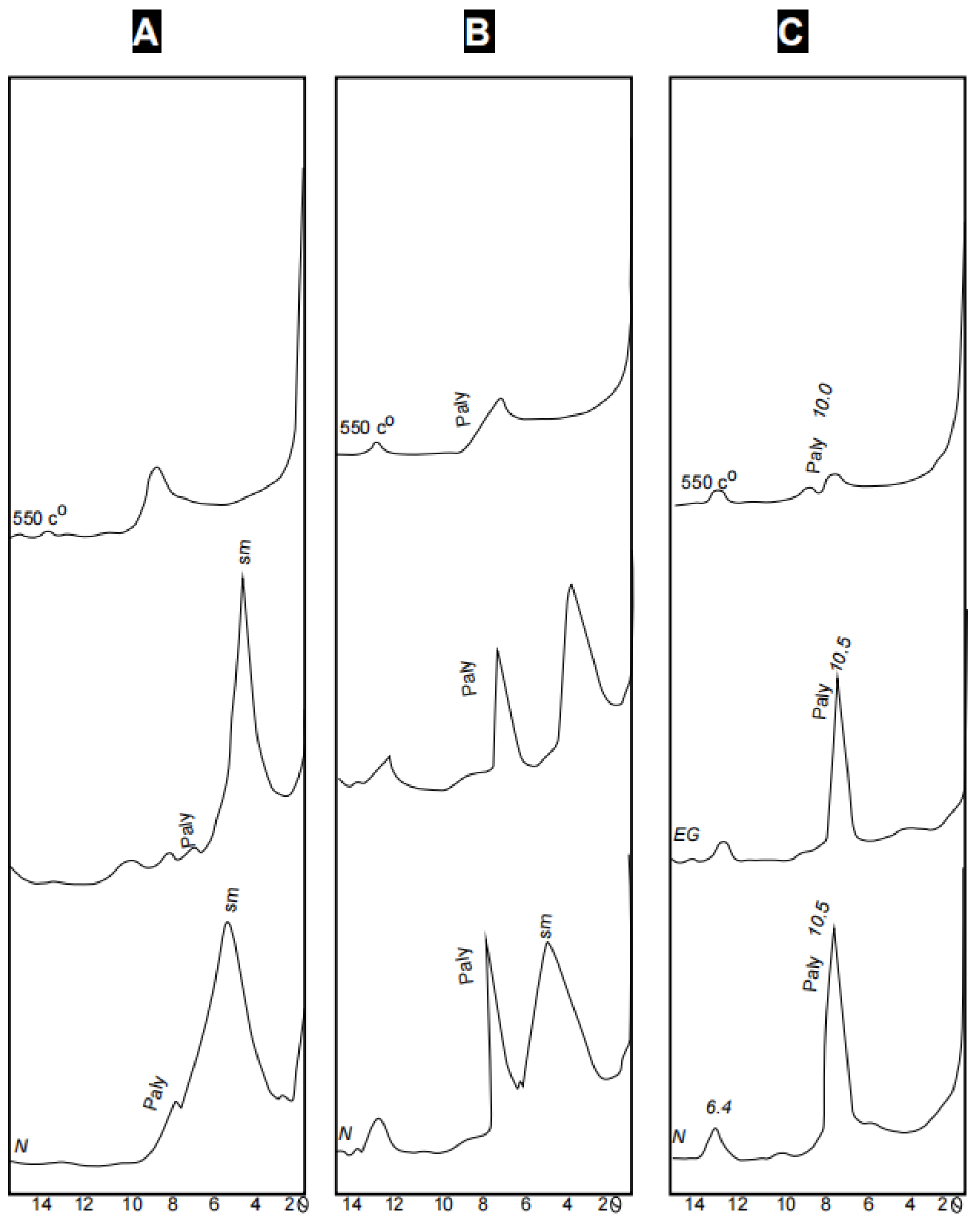

Fig.8. XRD of oriented clay fractions (N, EG, 550 °C) from Safra Member shales: A) lower shale sample is smectite-dominated, B) middle shale bed, smectite-palygorskite-dominated, C) whereas the upper shale sample is palygorskite-dominated

4. Discussion

4.1. Depositional Model

The depositional model based on facies, microfacies, and mineralogical data indicates that the Jeed Formation was deposited on a distally steepened marine ramp along the southern edge of the Tethys Ocean, and that a tectonically active basin developed west of the Ga'ara–Rutbah Region (Mohammed et al., 2022). The outer ramp was affected by upwelling currents that brought nutrients and silica, leading to the buildup of smectite-rich marl, carbonaceous shale, and spiculitic porcellanite under dysoxic to anoxic conditions. The mid–ramp underwent storm- and wave-driven reworking, producing mixed siliciclastic–phosphatic facies, including ooidal and peloidal phosphorite and a quartz–phosphate packstone. The inner ramp featured oyster banks, dolomitization, and palygorskite precipitation, indicating higher energy, shallower waters, and a more arid climate with occasional exposure to the sea. This model explains the vertical and lateral facies patterns seen in the Jeed Formation and their connection to changes in sea level and climate. The Jeed Formation is subdivided into four third-order depositional sequences (DS1-DS4), which are separated by five sequence boundaries (SB1-SB5). DS1 captures the initial Upper Maastrichtian transgression over the Tayarat Formation, characterized by a basal phosphorite lag and outer-ramp shale and porcellanite. DS2 includes the main Upper Maastrichtian maximum flooding and subsequent shallowing, indicated by condensed outer-ramp facies and overlying mid- and inner-ramp deposits. DS3 is a localized basal Danian sequence, preserved mainly in borehole BH5/6, where Early Danian facies rest directly on the K/Pg surface. DS4 records the major Danian transgressive-regressive cycle that formed most of the Trafawi Member, ending with inner-ramp facies and capped by the Danian-Selandian unconformity (SB5). SB1 marks the base of the Jeed over the Tayarat Formation, SB2 separates two Maastrichtian cycles within Safra, SB3 corresponds to the K/Pg boundary, SB4 indicates a Late Danian regressive surface, and SB5 signifies the regional hiatus at the top of the Jeed Formation. This framework aligns well with regional and global eustatic curves, a strong basis for interbasinal correlation (Fig. 9).

4.2. K/Pg unconformity and Regional Stratigraphic Correlation

The K/Pg unconformity in the Western Desert of Iraq is very clear and easily recognized in the field, separated by a phosphatic bed that divides the Safra Member from the above Trafawi Member of the Jeed Formation. This unconformity surface is characterized by firmground or hardground in some areas and displays an uneven, erosional shape. The western desert in Iraq, one of the more open-marine regions, shows an unconformity surface marked by highly intense bioturbation, mainly consisting of *Thalassinoides* burrow networks, suggesting that the seafloor was exposed for a long period before sedimentation resumed. The lag deposit, composed of reworked phosphatic fragments and pebbles, quartz grains, bivalve shell debris, and iron-rich nodules, is often seen lying above the boundary. This indicates a high-energy environment in which reworking occurred.

Biostratigraphic evidence indicates a short but regionally significant hiatus across this surface. The absence of the Early Danian planktonic foraminiferal zones P1a and P1b in many Western Desert sections suggests either non-deposition or erosion immediately following the latest Maastrichtian. This hiatus is consistent with a major reorganization of depositional environments at the end of the Cretaceous. It has been documented extensively along the southern boundary of the Tethys Ocean. In Jordan, a type of unconformity of this kind is found in the Muwaqqar Formation, which is characterized by erosion, condensation, and a sudden vertical facies change, indicating rapid paleoenvironmental shifts at the K/Pg boundary (Farouk et al., 2014).In the central and southern parts of Egypt, the Dakhla Formation shows a flat surface with distinct lithological contacts at the K/Pg transition, separating the Lower Khargra Member from the above Upper Khargha Member, with a similar break in deposition in the Western Desert of Iraq. Further east, an unconformable contact is observed in the Simsima Formation, which is overlain by the Paleocene Muthaymimah Formation in the UAE. In Saudi Arabia, the K/Pg unconformity is recognized in the Aruma Formation, separating the Maastrichtian Hajajah and Paleocene Lina Members, as evidenced by facies changes and stratigraphic truncation (Farouk et al., 2020). The Jeed Formation is stratigraphically on par with the Muwaqqar in Jordan and the Dakhla Shale in Egypt, as well as with other age-equivalent successions in the Levant Basin (Farouk, 2016 ; Farouk et al., 2020). Together, these units depict the Upper Maastrichtian to Danian outer-to-inner ramp deposition, where the main lithologies were phosphorite, organic-rich mud, chalk, porcellanite, and silicate interbeds. The stratigraphic alternations display a region-wide gap at the K/Pg boundary, followed by an Early Danian phosphogenic sea-level rise.

The regional continuity of these successions and their associated unconformities suggests the development of an extensive southern Tethyan phosphogenic belt extending from western Iraq through Jordan and into Egypt. This belt was influenced by the interaction of regional tectonics related to the Hail–Rutbah High and the Syrian Arc Fold System, nutrient-rich cold-water upwelling, greenhouse climatic conditions, and generally low sedimentation rates during the latest Cretaceous and earliest Paleogene.

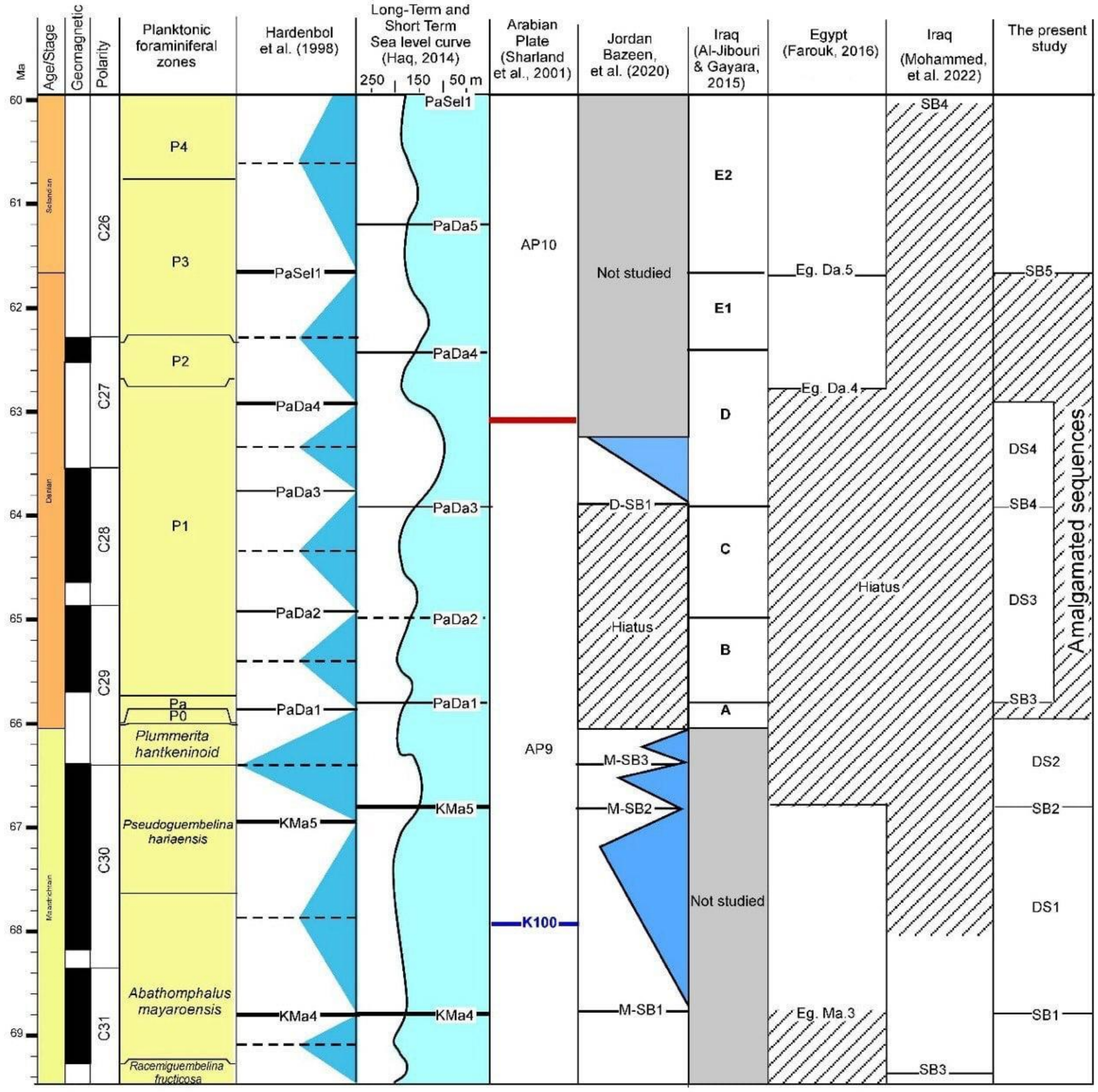

Fig. 9. Regional correlation of successions with the Arabian Plate (Sharland et al., 2001), the European Basin (Hardenbol et al., 1998), (Haq, 2014), and other regions within Jordan and Egypt

5. Conclusions

The main conclusion of the present study is:

- The Upper Maastrichtian-Lower Danian phosphatic-siliceous sequence in the Ga'ara-Rutbah region differs from the Upper Campanian-Lower Maastrichtian Digma Formation in geochronology, lithology, mineralogy, environment, and tectonic setting. Unlike the glauconitic, foraminifera-rich marly limestone of the Digma Formation, which was deposited in a deeper basinal setting, the Ga'ara–Rutbah succession contains phosphorite, porcellanite, chert, fossiliferous limestones, sandstone, and shale, with no glauconite. Consequently, the Digma Formation neither crops out nor occurs subsurface west of Rutbah, and the Jeed Formation is formally proposed for this succession.

- The Jeed Formation meets ICS criteria for a formation-level unit: it is laterally traceable, lithologically distinct, internally consistent, and marked by well-documented unconformities. Distinguishing the Jeed from the Upper Campanian-Lower Maastrichtian Digma Formation clarifies the age and depositional environment of the Upper Cretaceous-Paleogene succession in western Iraq, thereby enhancing regional correlation with neighboring countries. Therefore, it is recommended that future editions of the Iraqi stratigraphic lexicon officially recognize the Jeed Format and limit the use of the Digma Formation to its original deep-marine Campanian -Lower Maastrichtian deposits in the Anah Graben.
- The type section of the Jeed Formation is located at the confluence of Wadi Jeed and Wadi Trafawi, which provides the most complete and representative exposure of the succession. Other reference sections include Er-Rudhma Al-Safra, which lies east of the Akashat Phosphate Mine, and Wadi Jandili. These sections primarily document the Safra Member and are crucial for recording its lateral variability and facies evolution. For the Trafawi Member, Wadi Trafawi is the best type area because it exhibits the full stratigraphic succession.
- The Jeed Formation is defined as comprising the Safra and Trafawi members, each with a lower and upper bed. The Safra Member unconformably overlays the Tayarat Formation, commencing with a basal phosphatic lag, succeeded by phosphorite-porcellanite-limestone-shale sequences that document a change from outer-ramp, plankton-rich facies to inner-ramp, oyster-bearing deposits. Lateral facies comprise dolomitic shale, marl, and hybrid phosphatic arenites, whereas the clay mineralogy transitions from smectite–opal-CT to palygorskite–dolomite, indicating a shift from humid to semi-arid environments. The Trafawi Member distinctly overlays the K/Pg boundary, commencing with a phosphatic firmground and a lag abundant in intraclasts and Thalassinoides. The Lower Trafawi Bed consists of 5–6 cycles of phosphorite, porcellanite, and shale, signifying Danian transgression, whereas the Upper Bed documents a shallowing into bioturbated sandstone and karstified limestone. The smectite -rich clay mineral composition indicates a hot, humid climate.

Author contributions: CRediT

Declaration of Competing Interest

The authors declare that they have no competing financial interests or personal relationships that could influence the work reported in this study.

Funding sources

This research did not receive any specific grant from funding agencies in the public, commercial, or not-for-profit sector.

Data Availability

Data are available in a public repository.
The data supporting the findings of this study are available in the references list.

Acknowledgments

This study is based on fieldwork conducted at various times since 1983, with support from the Iraqi Geological Survey. Laboratory analyses were performed with assistance from the Department of Geology at the University of Baghdad. The authors are also grateful to Sahira Abdul Kareem, Fadhil Lawa, Majid Mutawalli, and Sherif Farouk for their valuable support with fossil identification, critical review, and constructive discussions, which significantly improved the quality of this research. We would also like to express our sincere appreciation to the reviewers for their valuable comments, which have significantly improved the manuscript. We are equally grateful to the Editor-in-Chief and the members of the editorial board for their efforts and support.

References

Abdel-Kireem, M. R., 1997. Contribution to the stratigraphy of the Upper Cretaceous and the Lower Tertiary of the Sulaimaniah-Dokan region, northeastern Iraq. Neues Jahrbuch für Geologie und Paläontologie - Abhandlungen, 172(1), 121–139. https://doi.org/10.1127/njgpa/172/1997/121

Abu Shama, A.M., Farouk, S.B., Abdelwahhab, A., Baze, Y.S., 2026. Foraminiferal biostratigraphy, paleoenvironmental interpretation, and sequence stratigraphy of the latest Maastrichtian–Thanetian succession in the Southern Galala Plateau, Eastern Desert, Egypt. Marine Micropaleontology, 203, 102555. https://doi.org/10.1016/j.marmicro.2026.102555

Al-Bassam, K.S., 2017. Development of the Phosphate Industry in Iraq: Resources, Requirements and Challenges. Iraqi Bulletin of Geology and Mining, Special Issue 7.

Al-Mutwaily, 1992. Planktonic foraminifera and biostratigraphy of the Digma Formation (Upper Cretaceous) in the Anah-1 borehole, Western Iraq. Journal of the Geological Society of Iraq.

Al-Naqib, K., 1967. Geology of the Arabian Peninsula - Southwestern Iraq. U.S. Geological Survey Professional Paper.

Arenillas, I., Alegret, L., Arz, J.A., Liesa, C., Meléndez, A., Molina, E., Soria, A.R., Cedillo-Pardo, E., Grajales-Nishimura, J.M., Rosales-Domínguez, C., 2002. Cretaceous-Tertiary boundary planktic foraminiferal mass extinction and biochronology at La Ceiba and Bochil, Mexico, and El Kef, Tunisia. Special Paper of the Geological Society of America. https://doi.org/10.1130/0-8137-2356-6.253

Bolli, H.M., 1966. Zonation of Cretaceous to Pliocene marine sediments based on planktonic foraminifera. Boletín Informativo de la Asociación Venezolana de Geología, Minería y Petróleo.

Buday, T., Hak, J., 1980. Report on geological survey of the western part of Iraq. GEOSURV, Internal Report, No.1000.

Canudo, J.I., Keller, G., Molina, E., 1991. Cretaceous/Tertiary boundary extinction pattern and faunal turnover at Agost and Caravaca, S.E. Spain. Marine Micropaleontology. https://doi.org/10.1016/0377-8398(91)90019-3

Catuneanu, O., 2017. Sequence stratigraphy: guidelines for a standard methodology. Stratigraphy & Timescales, 2, 1–57.

Chamley, H., 1989. Clay Formation Through Weathering. In Clay Sedimentology. Springer-Verlag, Berlin Heidelberg. https://doi.org/10.1007/978-3-642-85916-8_2

Dunham, R.J., 1962. Classification of carbonate rocks according to depositional texture. In: Ham, W.E. (Ed.), Classification of Carbonate Rocks. American Association of Petroleum Geologists Memoir 1, 108–121.

Embry, A.F., Klovan, J.E., 1971. A Late Devonian reef tract on northeastern Banks Island, NWT. Bulletin of Canadian Petroleum Geology, 19(4), 730–781.

El-Younsy, A.R.M., Obaidalla, N.A., Philobbos, E.R., Salman, A.M., 2017. High-resolution sequence stratigraphy of the Upper Cretaceous-Lower Paleogene succession, Gabal Qreiya area, Upper Egypt. Arabian Journal of Geosciences. https://doi.org/10.1007/s12517-017-3319-z

Farouk, S., Marzouk, A.M., Ahmad, F., 2014. The Cretaceous/Paleogene boundary in Jordan. Journal of Asian Earth Sciences, 94. https://doi.org/10.1016/j.jseaes.2014.08.015

Farouk, S., 2016. Paleocene stratigraphy in Egypt. Journal of African Earth Sciences, 113. https://doi.org/10.1016/j.jafrearsci.2015.10.013

Farouk, S., Al-Kahtany, K., Jain, S., Ahmad, F., El-Sorogy, A., 2020. Isotope stratigraphy (87Sr/86Sr, 13C) and depositional sequences of the Aruma Formation, Saudi Arabia: Implications to eustatic sea-level changes. Geological Journal. https://doi.org/10.1002/gj.3875

Haq, B.U., 2014. Cretaceous eustasy revisited. Global and Planetary Change, 113, 44–58. https://doi.org/10.1016/j.gloplacha.2013.12.007

Hardenbol, J., Thierry, J., Farley, M.B., Jacquin, T., de Graciansky, P.-C., Vail, P.R., 1998. Mesozoic and Cenozoic Sequence Chronostratigraphic Framework of European Basins. Mesozoic and Cenozoic Sequence Stratigraphy of European Basins, 3–13. https://doi.org/10.2110/pec.98.02.0003

Jassim, S.Z., Karim, S.A., Basi, M., Al-Mubarak, M.A., Munir, J., 1984. Stratigraphy. Manuscript report. Final Report on the Regional Geological Survey of Iraq, vol. 3. Geological Survey of Iraq.

Jassim, S.Z., Goff, J.C. (Eds.), 2006. Geology of Iraq. DOLIN, sro, distributed by the Geological Society of London.

Keller, G., 2004. Low-diversity, Late Maastrichtian and Early Danian planktic foraminiferal assemblages of the Eastern Tethys. Journal of Foraminiferal Research. https://doi.org/10.2113/0340049

Li, L., Keller, G., 1998a. Maastrichtian climate, productivity, and faunal turnovers in planktic foraminifera in South Atlantic DSDP sites 525A and 21. Marine Micropaleontology. https://doi.org/10.1016/S0377-8398(97)00027-3

Li, L., Keller, G., 1998b. Maastrichtian diversification of planktic foraminifera at El Kef and Elles, Tunisia. Eclogae Geologicae Helvetiae, 91, 75–102.

Mohammed, I.Q., Farouk, S., Mousa, A., Lawa, F.A., 2022. Lithofacies types, mineralogical assemblages, and depositional model of the Maastrichtian–Danian successions in the Western Desert of Iraq and eastern Jordan. Journal of African Earth Sciences. https://doi.org/10.1016/j.jafrearsci.2021.104397

Mousa, A.K., Al-Dulimi, S.I., Mohammed, I.Q., 2021. Microfacies analysis of the Late Maastrichtian-Danian Phosphatic Succession in the H3-Trebeel district, Western Desert of Iraq. Iraqi Journal of Science, 62(4), 1188–1203. https://doi.org/10.24996/ijs.2021.62.4.15

Premoli Silva, I., Sliter, W.V., 1995. Cretaceous planktonic foraminiferal biostratigraphy and evolutionary trends from the Bottaccione section, Gubbio, Italy. Palaeontographia Italica, 82, 1–89. https://doi.org/10.1130/0-8137-2332-9.301

Sharbazheri, K.M., 2007. Age of Unconformity within Tanjero Formation in Chwarta Area, Northeast of Iraq (Kurdistan Region). Iraqi National Journal of Earth Science (INJES). https://doi.org/10.33899/earth.2007.39402

Sharland, P.R., Archer, D.M., Casey, R.B., Davies, S.H., Hall, A.P., Heward, A.D., Horbury, A.D., Simmons, M.D., 2001. Arabian Plate Sequence Stratigraphy. GeoArabia Special Publications 2, 371.

Sissakian, V.K., Mohammed, B.S., 2007. Geology of Iraqi Western Desert (Stratigraphy). Special Issue. Iraqi Bulletin of Geology and Mining, 51–124.

Sissikian, V.K., Fouad, S.F., 2016. Geological Map of Iraq, scale 1:1,000,000. Iraq Geological Survey Publications.

Smit, J., 2005. The section of the Barranco del Gredero (Caravaca, SE Spain): A crucial site for the Cretaceous/Tertiary boundary impact-extinction hypothesis. Journal of Iberian Geology, 31(1), 179–191.

Van Bellen, R.C., Dunnington, H.V., Wetzel, R., Morton, D.M., 1959. Lexique Stratigraphique International: Asie, Fascicule 10a, Irak. Centre National de la Recherche Scientifique.

Wade, B.S., Pearson, P.N., Berggren, W.A., Pälzke, H., 2011. Review and revision of Cenozoic tropical planktonic foraminiferal biostratigraphy and calibration to the geomagnetic polarity and astronomical time scale. Earth-Science Reviews, 104(1–3), 111–142. https://doi.org/10.1016/j.earscirev.2010.11.004